Article

High-sensitive electrochemiluminescence C-peptide biosensor via the double quenching of dopamine to the novel Ru(II)-organic complex with dual intra-molecular self-catalysis

Haijun Wang, Liyu Peng, Ya-Qin Chai, and Ruo Yuan

Anal. Chem., **Just Accepted Manuscript** • DOI: 10.1021/acs.analchem.7b03125 • Publication Date (Web): 26 Sep 2017

High-sensitive electrochemiluminescence C-peptide biosensor via the double quenching of dopamine to the novel Ru(II)-organic complex with dual intra-molecular self-catalysis

Haijun Wang*[1], Liyu Peng[2], Yaqin Chai[1], Ruo Yuan*[1]

[1]Key Laboratory of Luminescent and Real-Time Analytical Chemistry (Southwest University), Ministry of Education, College of Chemistry and Chemical Engineering, Southwest University, Chongqing 400715, PR China; [2]Faculty of Engineering, Department of materials, Imperial College London, United Kingdom

* Corresponding author: Tel.: +86-23-68252277; Fax: +86-23-68253172.

E-mail address: hjwang@swu.edu.cn, yuanruo@swu.edu.cn

ABSTRACT

Here, a novel Ru(II)-organic complex (Ru-PEI-ABEI) with high electrochemiluminescence (ECL) efficiency was proposed to construct a sensitive quenching-typed ECL biosensor for C-peptide (C-P) measurement based on the double quenching effect of dopamine (DA). The high ECL efficiency of Ru-PEI-ABEI was originated from the dual intra-molecular self-catalysis including intra-molecular co-reaction between polyethyleneimine (PEI) and $Ru(bpy)_2(mcbpy)^{2+}$, and intra-molecular ECL resonance energy transfer (ECL-RET) from N-(aminobutyl)-N-(ethylisoluminol) (ABEI) to $Ru(bpy)_2(mcbpy)^{2+}$, which would generate a strong initial ECL signal. Through sandwiched immunoreaction and 3D DNA walking machine, a certain amount of target C-P was converted to a large amount of intermediate DNA that could further trigger hybridization chain reaction

(HCR) to introduce into massive DA which not only could quench the ECL of $Ru(bpy)_2(mcbpy)^{2+}$, but also quench the ECL of ABEI. Thus, the double quenching effect of DA would effectively quench the ECL of Ru-PEI-ABEI, leading to an obviously decreased final ECL signal. Thus, a sensitive quenching-typed ECL biosensor was constructed for C-P detection with a linear range from 50 fg mL^{-1} to 16 ng mL^{-1} and an estimated detection limit of 16.7 fg mL^{-1}. The dual intra-molecular self-catalyzed strategy and the double quenching strategy based on one quencher to the same luminous reagent proposed in this work would provide new thought in both ECL signal enhancement and quenching efficiency improvement.

KEYWORDS

Electrochemiluminescence; intra-molecular co-reaction; intra-molecular RET; double quenching; biosensor

INTRODUCTION

C-peptide (C-P) with 31 amino acids is a cleavage product of proinsulin released from pancreatic beta cells.[1] It has been proven to be a useful marker to assess diabetes mellitus and its complications, such as nerve damage, kidney disease, foot disease and blindness, suggesting the remarkable significance of the sensitive and accurate detection for C-P.[2] In 1970, the first radioimmunoassay (RIA) for C-P was reported.[3] However, this method is time-consuming, harmful to the operator, easy to be interfered and often inaccurate. After that, although there have some developments for C-P assays, imperious demands are still needed in improvement of sensitivity and accuracy.[4,5] Electrochemiluminescence (ECL), a popular and favorable analytical technique with many merits, for instance simplified optical setup,

outstanding controllability and high sensitivity, has been attracting increasing attention, which possesses immense potential for sensitive C-P detection.[6-8]

Currently, many analytical models of ECL biosensors (such as ratiometric model and signal enhanced model) are proposed, in which quenching-typed ECL biosensor is one of the most important for ECL technique.[9,10] Two fundamental factors directly limit the wider application of this ECL detected model. The primary one is the initial ECL signal, which is mainly related to the ECL efficiency of luminophores. Many studies indicate that ECL co-reaction and ECL resonance energy transfer (ECL-RET) are the most effective ways for improving the luminophore's efficiency.[11,12] It has been also confirmed that both intra-molecular ECL co-reaction and intra-molecular ECL-RET would induce higher ECL efficiency and stability compared with that of traditional inter-molecular interactions due to the shortened electronic transmission distance and reduced energy loss.[13,14] However, the concerted enhancement combined intra-molecular co-reaction with intra-molecular RET in the same luminous molecular almost has not been reported, by which the ECL efficiency can be further greatly improved compared to the individual intra-molecular co-reaction or individual intra-molecular ECL-RET. Here, a novel Ru(II)-organic complex (Ru-PEI-ABEI) was proposed by using $Ru(bpy)_2(mcbpy)^{2+}$ (as energy accepter) to simultaneously covalently connect with N-(aminobutyl)-N-(ethylisoluminol) (ABEI, as energy donor) and polyethyleneimine (PEI, as co-reactant for both $Ru(bpy)_2(mcbpy)^{2+}$ and ABEI), exhibiting extremely high ECL efficiency and stability owing to the dual intra-molecular self-catalysis including intra-molecular co-reaction and intra-molecular ECL-RET.

Another key factor is the quench efficiency of the quencher introduced into the ECL

biosensors. Up to now, various quenchers for the ECL of Ru(II)-based complexes have been involved in the fabrication of ECL biosensors. Xu's group fabricated an ECL biosensor for DNA detection through in situ generating H_2O_2 by enzyme reaction to quench the ECL signal of $Ru(bpy)_3^{2+}$.[15] Wu and Wei's group used nanomaterial of $NiCo_2S_4$ to quench the ECL of $Ru(bpy)_3^{2+}$, by which a biosensor for Con A detection was constructed.[16] In addition, ferrocene (Fc) as a classical quencher for ECL of Ru(II)-based complex was widely applied in the ECL analysis.[17,18] However, the quench efficiency in most of these previous approaches still requires further improvement. Here, massive dopamine (DA) introduced by nucleic acid technique was used to quench the ECL of the newly prepared Ru-PEI-ABEI. In particularly, DA not only could directly quench the ECL of Ru(II) complex, but also quench the ECL of ABEI, resulting in an outstanding quench efficiency. The proposed double quenching strategy based on one quencher to the same luminous reagent is first reported, which would lead to higher sensitivity for quenching-typed ECL biosensor and broaden the application of ECL technology.

Meanwhile, to further enhance the detection sensitivity in the construction of ECL biosensors, some auxiliary strategies are usually included, and the most important of them is the nucleic acid amplified technique, such as polymerase chain reaction (PCR) and rolling circle amplification (RCA).[19-21] Recently, DNA nanotechnology has aroused much attention, and many well-defined DNA nanostructures with excellent properties have been extensively investigated, for instance, tetrahedrons, nanotubes, and nanotweezers.[22-24] Among them, DNA walking machine, an artificial molecular machine with high self-assembly efficiency and cargoes handling capacity, attracts increasing interest.[25] Especially, a newly reported

three-dimensional (3D) DNA walking machine with more sufficient walking space and payload releasing would possess wider application compared with traditional one-dimensional (1D) or two-dimensional (2D) DNA walking machines.[26] Here, we intend to induce 3D DNA walking machine combined with hybridization chain reaction (HCR) into the construction of quenching-typed ECL biosensor for efficient target conversion and enhancement of loading amount of quencher, resulting in ultrahigh detection sensitivity.

Herein, a novel Ru(II)-organic complex (Ru-PEI-ABEI) was prepared by simultaneously covalently coupling $Ru(bpy)_2(mcbpy)^{2+}$ (also as energy transfer accepter) with co-reactant polyethyleneimine (PEI) and corresponding energy transfer donor N-(aminobutyl)-N-(ethylisoluminol) (ABEI). The obtained Ru-PEI-ABEI possessed high ECL efficiency because of the dual intra-molecular self-catalysis, including intra-molecular co-reaction between PEI and $Ru(bpy)_2(mcbpy)^{2+}$ and intra-molecular ECL-RET from ABEI to $Ru(bpy)_2(mcbpy)^{2+}$. When Ru-PEI-ABEI was modified onto the electrode, a strong initial ECL signal was produced. Then, the 3D DNA walking machine was prepared by using convex hexoctahedral Pd@Au core-shell nanocrystals (Pd-Au HOHs) to immobilize abundant DNA walker probe, support probe 1 (S1), and the secondary antibody (Ab_2). At the presence of C-P, an immune complex was acquired through the sandwiched immunoreaction between Ab_2 immobilized on Pd-Au HOHs and the first antibody (Ab_1) loaded on the Au nanoparticles functionalized Fe_3O_4 (Au@ Fe_3O_4). As the DNA walker probe paired with S1, a recognition site for nicking endonuclease (Nb.BvCI) appeared. Therefore, under the shearing of Nb.BvCI, the intermediate DNA would be produced accompany with the releasing of DNA walker probe which would pair with the next S1 and undergo a further releasing process again. In that

way, a certain amount of target C-P was converted to a large amount of intermediate DNA in solution. Furthermore, the obtained intermediate DNA could further trigger the HCR on the electrode to introduce massive DA. Coincidentally, DA not only could quench the ECL of $Ru(bpy)_2(mcbpy)^{2+}$, but also quench the ECL of ABEI, which would cause a high quenching efficiency to the ECL of Ru-PEI-ABEI, resulting in an obvious decreased ECL signal. And the quenching effect would increase with increasing the concentration of C-P, based on which a sensitive quenching-typed ECL biosensor was constructed. The preparation of intermediate DNA, the construction of the biosensor and the signal enhanced mechanism were presented in scheme 1. The strategies proposed in this work offers new means for ECL signal enhancement, ECL quenching efficency improvement, and possible early diagnosis and treatment for C-P related disease.

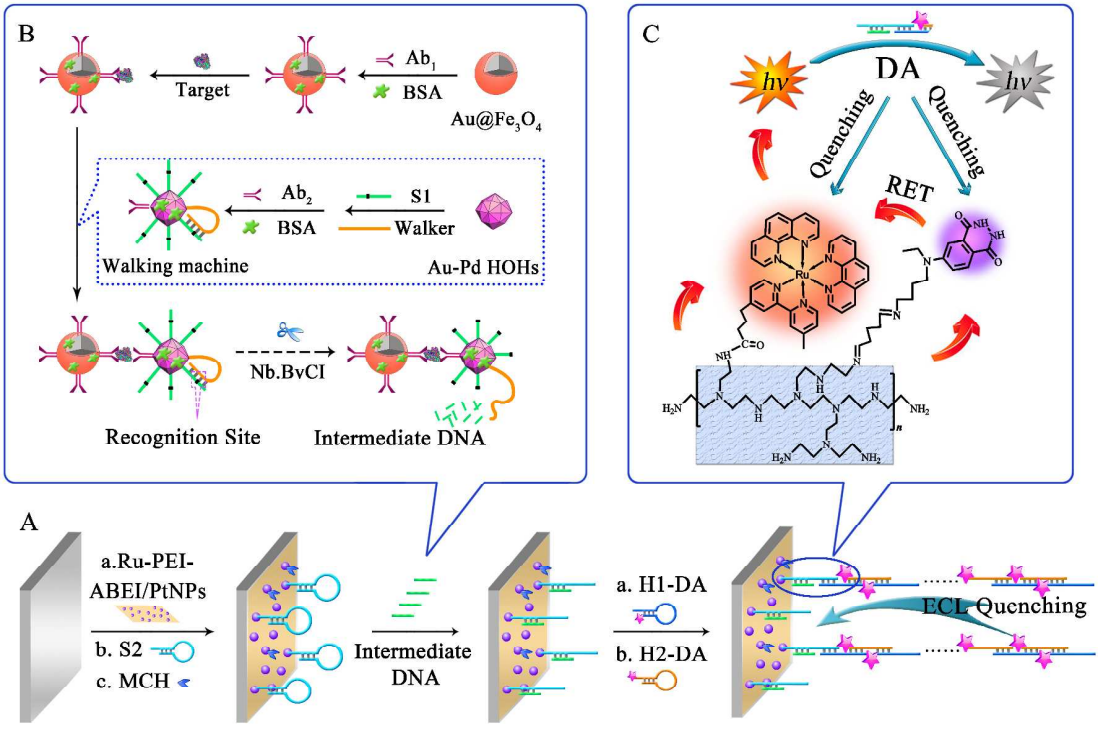

Scheme 1 The construction of the biosensor (A), the preparation of intermediate DNA (B)

and the signal enhanced and quenched mechanism (C)

EXPERIMENTAL SECTION

Reagents and apparatus. Carcinoembryonic antigen (CEA), Prostate specific antigen (PSA), C-peptide (C-P) and its antibody were purchased from Biocell Company (Zhengzhou, China). Bis(2, 2'-bipyridyl)(4'-Methyl-[2, 2']bipyridinyl-4-carboxylicacid) ruthenium (Ⅱ) dichloride ($Ru(bpy)_2(mcbpy)^{2+}$), N-(aminobutyl)-N-(ethylisoluminol) (ABEI) and poly(ethylenimine) (PEI, 50%) were acquired from Suna Tech Inc. (Suzhou, China), TCI Development Co., Ltd. (Shanghai, China) and Fluka (Switzerland), respectively. Potassium tetra-chloropalladate (K_2PdCl_4), gold chloride tetrahydrate ($HAuCl_4 \cdot 4H_2O$), N-Hydroxy succinimide (NHS), N-(3-Dimethylaminopropyl)-N′-ethylcarbodiimide hydrochloride (EDC), bovine serum albumin (BSA, 96-99%) and glutaric dialdehyde (GA, 50%) were got from Sigma-Aldrich Chem. Co. (St. Louis, MO, USA). From Shanghai Chemical Reagent Company (Shanghai, China), ascorbic acid (AA) was acquired. Both cetyltrimethylammonium bromide (CTAB) and cetylpyridinium chloride monohydrate (CPC) were purchased in Kelong Chemical Company (Chengdu, China). The human serum speciments for C-P were acquired from Southwest Hospital in Chongqing of China. Phosphate-buffered solution (PBS) (pH 8.0, 0.1 M) used in this work contained Na_2HPO_4 (0.1 M), KH_2PO_4 (0.1 M), and KCl (0.1 M). The oligonucleotides used in this work were listed Table S1 in the Supporting Information, which were prepared by Shanghai Sangon Biological Engineering Technology and Services Co., Ltd. (Shanghai, China).

The classical three-electrode system that used the modified glassy carbon electrode (GCE) as working electrode, Ag/AgCl (sat. KCl) as reference electrode and platinum wire as

counter electrode, was involved in ECL detection. ECL measurement was performed on MPI-E ECL analyzer from Xi'an Remax Electronic science & Technology Co.Ltd. (Xi'an, China). Meanwhile, the potential scanning from 0.2 to 1.25 V and the voltage of photomultiplier tube (PTM) set at 800 V were applied in ECL detection. The F7000 fluorescence spectrophotometer (Hitachi High-TechScience Co., Tokyo, Japan) was used for photoluminescence property study. Furthermore, both the transmission electron microscope (TEM, H600, Hitachi Instrument, Japan) and Scanning electron microscopy (SEM, S-4800, Hitachi, Japan) were applied for material characterization.

Preparation of 3D DNA walking machine and intermediate DNA. First of all, convex Au-Pd HOHs were prepared according to the literature with minor modifications,[27] and the details were presented in the Supporting Information. Then, the DNA walker probe (0.5 μM), support probe 1 (S1, 5μM) were successively added into the obtained Au-Pd HOHs solution (1 mL). Trough Au-S/Pd-S bond, the DNA walker and S1 functionalized Au-Pd HOHs were obtained by centrifugation and washing. And the DNA walker could pair with the nearby S1 through base complementary pairing. Then, the secondary antibody (Ab_2, 200 μL) was further dropped into the solution of Au-Pd HOHs-walker-S1 (2 mL), and the obtained mixture solution was placed at 4°C with constant stirring overnight. After centrifugation and washing, the Au-Pd HOHs-walker-S1@ Ab_2 was acquired. To block the nonspecific adsorption sites, BSA (1 mL) was mixed with the obtained solution of Au-Pd HOHs-walker-S1@ Ab_2 (1 mL) with constant stirring for 1 h. After discarding the excess reagents through further centrifugation and washing, the Au-Pd HOHs-walker-S1@Ab_2/BSA bioconjugate, also named 3D DNA walking machine, was acquired. In addition, Au nanoparticles functionalized Fe_3O_4

($Au@Fe_3O_4$, 2 mL) was used as platform to load the first antibody (Ab_1, 200 μL). By using BSA to block the nonspecific adsorption sites, the $Au@Fe_3O_4@Ab_1$/BSA bioconjugate was obtained by magnetic separation and washing.

At the presence of C-P, through the sandwiched immunoreaction, an immune complex ($Au@Fe_3O_4@Ab_1$/BSA/C-P/Au-Pd HOHs-walker-S1@Ab_2/BSA) was acquired by magnetic separation. When the DNA walker probe paired with S1, a recognition site for nicking endonuclease (Nb.BvCI) appeared. Therefore, the intermediate DNA would be produced after the cutting by Nb.BvCI (5 U) accompany with the releasing of DNA walker probe which would pair with the next S1 and undergo a further releasing process again. In this way, the DNA walker probe would walk from near to far along the 3D surface of Au-Pd HOHs, and a large amount of intermediate DNA would be obtained through magnetic separation owing to high local concentration of DNA components and the wide 3D walking space. The preparation of the 3D DNA walking machine and intermediate DNA was presented in scheme 1 B.

Fabrication of the ECL biosensor. Firstly, by being polished with alumina slurry (0.3, 0.05 mm), rinsed thoroughly with deionized water and further sonicated in ethanol, deionized water respectively, the cleaned GCE (Φ = 4 mm) was obtained. 5 μL Ru-PEI-ABEI/PtNPs (seen in the Supporting Information for the preparation details) dispersed in nafion solution (0.25%) was dropped onto the cleaned GCE, and a film was formed after drying in air. Then, the support probe 2 (S2, 2 μM) was coated on the electrode through Pt-S bond, and MCH was further used to block the nonspecific adsorption sites for 2 h. After washing, the obtained solution of intermediate DNA (10 μL) was incubated on the modified electrode for 2 h.

Finally, the modified electrode was incubated with the mixture of hairpin probe H1 (5 μL, 1 μM) and H2 (5 μL, 1 μM) which were both marked by dopamine (DA) through the amide reaction with the assistance of EDC and NHS. With increasing the concentrations of C-P, an increased amount of intermediate DNA would be produced, which would trigger the HCR reaction more effectively and further introduce into more DA for more effective ECL quenching. Therefore, the final ECL intensity was well negatively correlated with the concentration of C-P, by which C-P could be monitored with high sensitivity and accuracy. The fabrication process for the biosensor and corresponding signal amplification and quenching mechanism were showed in scheme 1 A and C.

Measurement procedure. For detection, C-P with different concentrations were used for sandwiched immunoreactions. And then, the as-prepared ECL biosensors were placed in an ECL detector cell containing PBS (3 mL) with the potential scanning from 0.2 to 1.25 V and the PTM being set at 800 V in the detection process. As the concentration of C-P increased, the amount of intermediate DNA increased, and then DA immobilized on the electrode increased accordingly, leading to more obvious decline of the ECL signals. Thus, the ECL signal changes directly reflected the concentration changes of C-P, by which C-P could be detected sensitively.

RESULTS AND DISCUSSION

Morphology characterization of Au-Pd HOHs. Au-Pd HOHs, as a key platform for preparation of 3D DNA walking machine, were characterized by TEM and SEM. At first, SEM image presented in Figure 1 A showed that Au-Pd HOHs possessed obvious polyhedral

shape in homogeneous distribution with a diameter of 110 ± 5 nm. Furthermore, TEM was used for further characterization, and the obtained image showed in Figure 1 B was similar with the results of SEM characterization above, illustrating the successful preparation of Au-Pd HOHs. Moreover, all the acquired results were good consistent with the those of the literature,[27] which further demonstrated the successful preparation of Au-Pd HOHs.

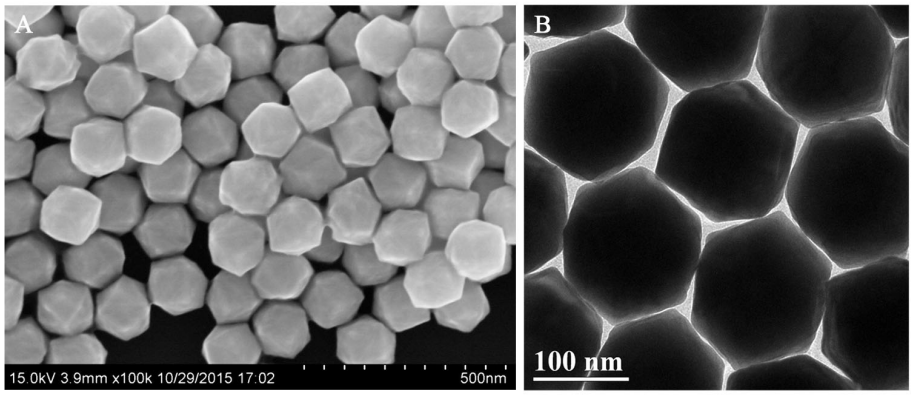

Figure 1. The SEM (A) and TEM (B) characterization for Au-Pd HOHs

Photoluminescence property of ABEI and $Ru(bpy)_2(mcbpy)^{2+}$.

As we mentioned above, the intra-molecular ECL-RET from ABEI to $Ru(bpy)_2(mcbpy)^{2+}$ was a very important aspect to the final high ECL efficiency of Ru-PEI-ABEI. In order to confirm potential possibility of ECL-RET between ABEI (Donor) and $Ru(bpy)_2(mcbpy)^{2+}$ (Acceptor), the photoluminescence (FL) spectra of them was monitored. From Figure 2, the maximum of FL excitation (Ex) spectrum and the FL emission (Em) spectrum for ABEI were 377.4 nm and 433.8 nm, respectively. And the maximum of FL Ex spectrum and the FL Em spectrum for $Ru(bpy)_2(mcbpy)^{2+}$ were 492.8 nm and 605.2 nm. There was an obvious overlapping between the FL Em spectrum of ABEI and the FL Ex spectrum of $Ru(bpy)_2(mcbpy)^{2+}$, illustrating good potentiality of ECL-RET from ABEI (Donor) to $Ru(bpy)_2(mcbpy)^{2+}$ (Acceptor).

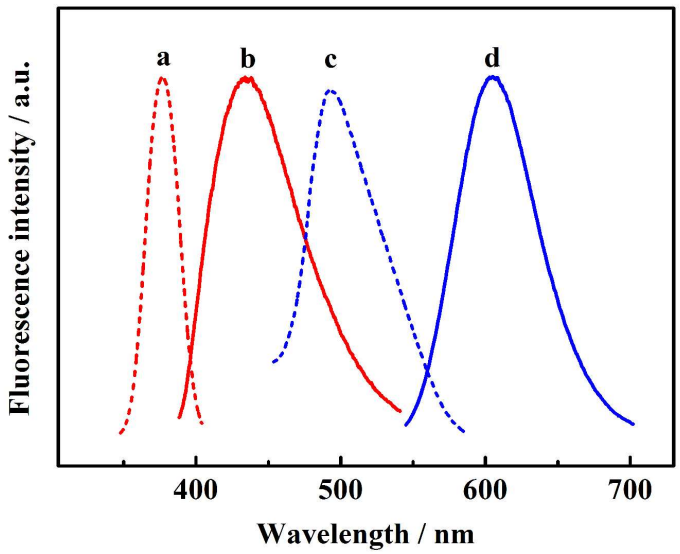

Figure 2. FL excitation spectrum for ABEI (a) and $Ru(bpy)_2(mcbpy)^{2+}$ (c), and FL emission spectrum for ABEI (b) and $Ru(bpy)_2(mcbpy)^{2+}$ (d)

Characterization of the fabricated process of the ECL biosensor. It has been proven that electrochemical impedance spectroscopy (EIS) is a useful way for the fabrication characterization of the biosensor. The EIS profiles for the stepwise modified process of the electrode were recorded in $[Fe(CN)_6]^{4-/3-}$ (5 mM) solution containing KCl (0.1 M). As presented in Figure 3, there was a small impedance value for the bare GEC (curve a). Then, the value increased obviously after the modification of Ru-PEI-ABEI-PtNPs dispersed with nafion solution which could effectively hinder the electron transfer (curve b). After that, the impedance values kept increasing when S2, MCH, intermediate DNA and the mixture of H1-DA and H2-DA were continuously modified onto the electrode (curve c, d, e and f). The reason was that the negatively charged DNA would hinder the diffusion of the negatively charged $[Fe(CN)_6]^{4-/3-}$ towards to the electrode surface, leading to the hindrance of electron transfer and increasement of the impedance value. The results obtained above demonstrated the successful fabrication of the biosensor.

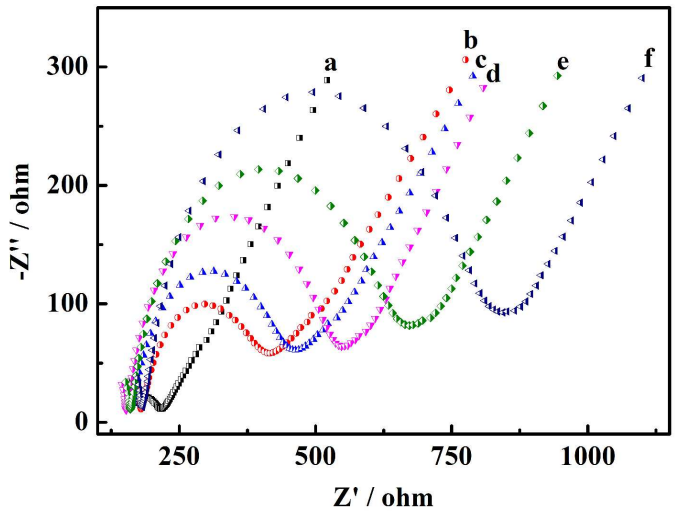

Figure 3. EIS profiles of bare GCE (a), GCE/Ru-PEI-ABEI-PtNPs (dispersed in nafion solution) (b), GCE/Ru-PEI-ABEI-PtNPs/S2 (c), GCE/Ru-PEI-ABEI-PtNPs/S2/MCH (d), GCE/Ru-PEI-ABEI-PtNPs/S2/MCH/Intermediate DNA (e), and GCE/Ru-PEI-ABEI-PtNPs/S2/MCH/Intermediate DNA/H1-DA-H2-DA (f) in $[Fe(CN)_6]^{4-/3-}$ (5 mM) containing KCl (0.1 M).

ECL behaviors of the quenching process. The quenching efficiency of DA induced by HCR was a key factor for the sensitivity of the proposed biosensor. For confirming this, the ECL behaviors were monitored. According to Figure 4, a high ECL signal (9656.1 a.u.) of the electrode before the modification of the intermediate DNA originated from the target (1 ng mL^{-1} C-P) conversion through 3D DNA walking machine was obtained (curve a). Then, the intermediate DNA was modified onto the electrode, which could trigger HCR and introduced into large amount of DA. Thus, an obvious decreased ECL signal (2396.8 a.u.) appeared because of the double quenching effect of DA to the luminous Ru-PEI-ABEI (curve b). The about 75% decline illustrated the effectiveness of the proposed strategy of the 3D DNA walking machine induced target conversion and the excellent quenching efficiency of DA

introduced by HCR.

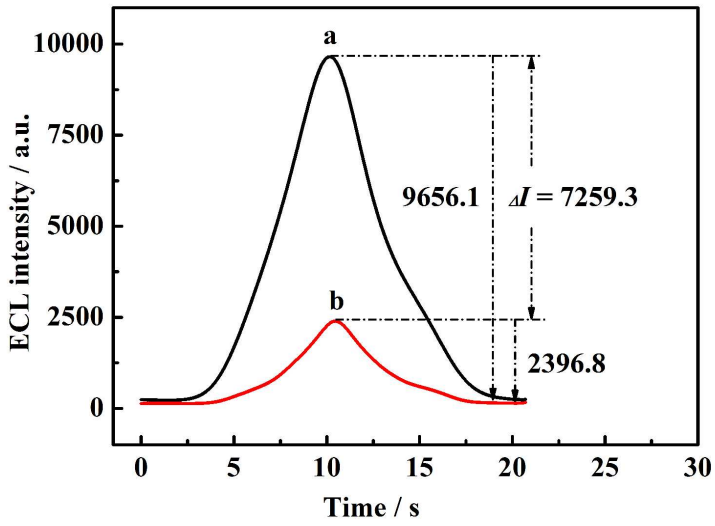

Figure 4. ECL behaviors of the modified electrode before the modification of intermediate DNA (a), and after the modification of intermediate DNA and HCR (b)

Analytical performance of the obtained biosensor for C-P detection. Under the optimal experimental condition (Figure S5 listed in Supporting Information), the analytical performance for the obtained biosensor was investigated by incubating C-P with various concentrations. The results were presented in Figure 5. Firstly, the ECL signal declined in turn as the concentration of C-P increased (Figure 5A, curve a-g). And then, The ECL intensities exhibited an outstanding linear relationship with the logarithm of C-P concentration. As seen from Figure 5B, the linear equation was I = 2383.4 - 1303.4 lg c (I represented the ECL intensity and c represented the concentration of C-P), and the correlation coefficient was 0.9991. The estimated limit of detection (LOD) (defined as LOD = $3S_B/m$, where m was the slope of the corresponding calibration curve and S_B was the standard deviation of the blank[28]) was 16.7 fg mL^{-1}, which was better than that of the previous reports (Table 1), demonstrating the favorable potentiality of this proposed biosensor in bioassays.[29-32]

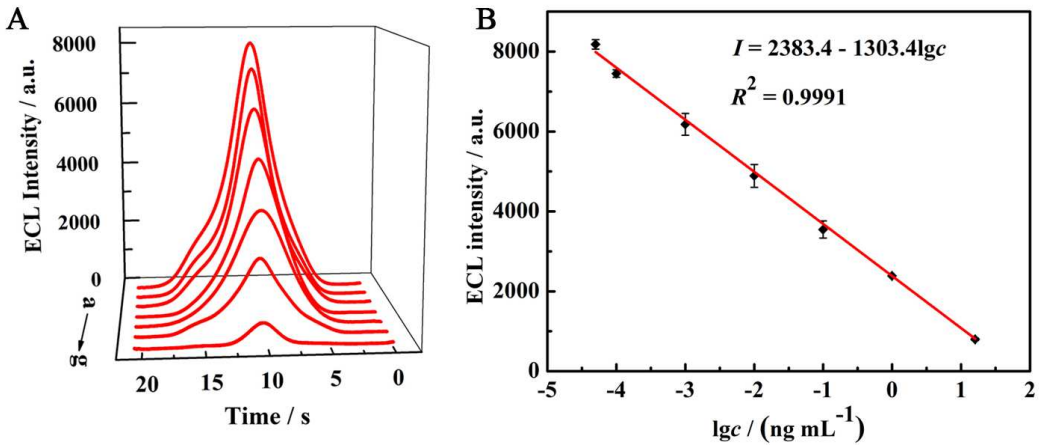

Figure 5. ECL intensities of the biosensor incubated with C-P of different concentrations of (a-g): 0.00005, 0.0001, 0.001, 0.01, 0.1, 1 and 16 ng mL^{-1} (A). Linear equation of the biosensor for C-P detection (B). All the ECL signals were detected in PBS (0.1 M, pH 8.0). The PTM was set at 800 V and the potential scan was from 0.2 to 1.25 V.

Table 1. Comparison of the present research with the previous works

Method	Target	Detection limit	References
Electrochemiluminescence	*N*-acetyl-*β*-D-glucosaminidase	0.17 pg mL^{-1}	29
Electrochemiluminescence	Antitransglutaminase type-2 antibodies	0.5 ng mL^{-1}	30
Quartz crystal microbalance	Thrombomodulin	2 ng mL^{-1}	31
Immunochromatographic assay	Ochratoxin A	0.085 ng mL^{-1}	32
Electrochemiluminescence	C-P	16.7 fg mL^{-1}	This work

Stability of the obtained biosensor. Stability was one of the most important properties of biosensors. To evaluate the stability of this proposed biosensor, the ECL intensities of the biosensor with different concentrations of C-P (1 and 0.1 ng mL^{-1}) under consecutive cyclic

potential scans were monitored. As seen from Figure 6, both the ECL intensities displayed no obvious change under 12 cycle potential scans, demonstrating the excellent stability of the obtained biosensor.

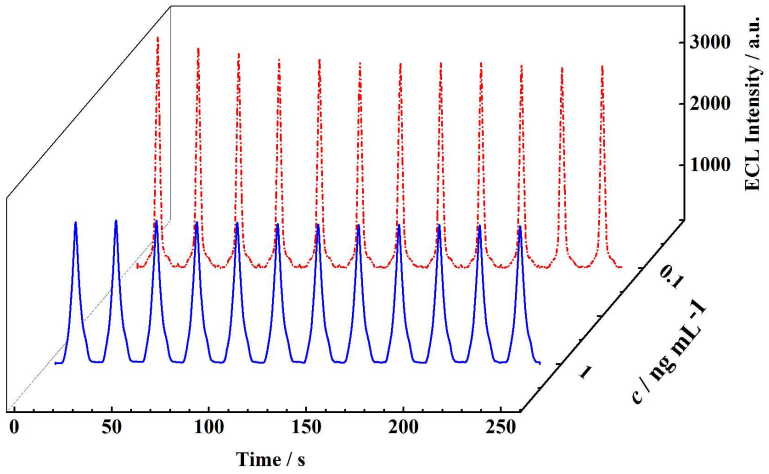

Figure 6. The stability of the biosensor incubated with C-P of different concentration (1 and 0.1 ng mL^{-1}) under consecutive cyclic potential scans

Selectivity and reproducibility of the obtained biosensor.

Meanwhile, the selectivity and reproducibility of this proposed biosensor were further investigated. Firstly, two interference reagents (CEA and PSA) were selected to perform comparative experiment for assessing the selectivity of this obtained biosensor. As shown in Figure 7, a high ECL signal of the biosensor incubated with CEA (5 ng mL^{-1}) appeared, which was almost the same with that of the blank sample. Moreover, the ECL intensities of the biosensor with the mixtures (Mix 1: C-P (0.1 ng mL^{-1}) and CEA (5 ng mL^{-1}); Mix 2: C-P (0.1 ng mL^{-1}), CEA (5 ng mL^{-1}) and PSA (5 ng mL^{-1})) kept similar with that of the pure C-P (0.1 ng mL^{-1}). All the results above illustrated that the proposed biosensor possessed excellent selectivity, which would have a good promising in clinical application. Furthermore, to evaluate the reproducibility of the biosensor, intra- and inter-assays were performed. The ECL

responses of biosensor prepared in four different batches were used to assess the inter-variation, and the ECL responses of four biosensors prepared in the same batch were used to assess the intra-variation. According to Figure S6 showed in Supporting Information, the calculated RSD of inter- and intra-assays were 4.74% and 3.78%, illustrating the outstanding reproducibility of the biosensor and the detected accuracy.

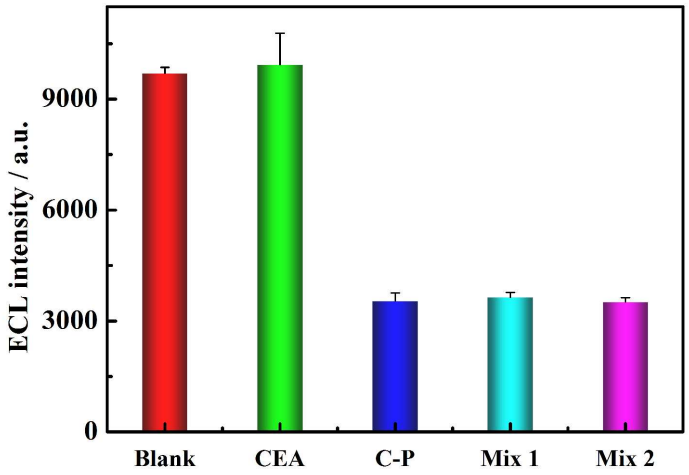

Figure 7. The ECL intensities of the biosensor with different targets: Blank; CEA (5 ng mL^{-1}); C-P (0.1 ng mL^{-1}); Mix 1: C-P (0.1 ng mL^{-1}) and CEA (5 ng mL^{-1}); Mix 2: C-P (0.1 ng mL^{-1}), CEA (5 ng mL^{-1}) and PSA (5 ng mL^{-1}).

Application of the proposed biosensor. In order to evaluate the potential possibility in clinical application, C-P with several concentrations (actual concentration) in human serum was detected by the proposed biosensor. And the recovery, defined as the ratio between the detected concentration and the actual concentration, was used to assess the analytical accuracy. The obtained recoveries, as presented in Table 2, were from 95.5% to 105%, suggesting the outstanding possibility in clinical application for the obtained biosensor.

Table 2. Measurement of C-P with different concentration in human serum

Sample number	Actual/ng mL^{-1}	Detected/ng mL^{-1} (n = 3)	Recovery/%
1	16.0	16.8	105
2	1.00	0.976	97.6
3	0.100	0.0955	95.5

CONCLUSIONS

In summary, a sensitive quenching-typed ECL biosensor for C-P detection was constructed. Two main strategies were designed to improve the detected sensitivity. Firstly, Ru-PEI-ABEI, as a novel luminous reagent, possessed high ECL efficiency owing to the dual intra-molecular self-catalysis including intra-molecular co-reaction and intra-molecular ECL-RET, generated a high initial ECL signal for the quenching-typed ECL biosensor. Secondly, on the basis of 3D DNA walking machine induced target conversion and intermediate DNA triggered HCR, large amount of DA with effective double quenching effect to the ECL of the obtained Ru-PEI-ABEI, was introduced to make an obviously decreased final ECL signal. Both the high enhancement of the initial ECL signal and effective decrease of the final ECL signal induced by target actualized the ultra-sensitive detection of the proposed quenching-typed biosensor. The strategies proposed in this work provided new thought in sensitivity improvement of quenching-typed ECL biosensor, including initial ECL signal enhancement and final ECL signal decrease. Moreover, the proposed biosensor held new promising in early diagnosis and treatment for C-P related disease.

ASSOCIATED CONTENT

Supporting Information

Preparation of convex Au-Pd HOHs and Ru-PEI-ABEI/PtNPs, characterization for Ru-PEI-ABEI, study of the dual intra-molecular self-catalysis of Ru-PEI-ABEI and the

double quenching effect of DA, optimal conditions of the ECL biosensor (Figure S1) and reproducibility of the biosensor (Figure S2)

AUTHOR INFORMATION

*** Corresponding authors**

Tel.: +86 23 68252277, fax: +86 23 68253172.

E-mail addresses: hjwang@swu.edu.cn, yuanruo@swu.edu.cn.

Notes

The authors declare no competing financial interest.

ACKNOWLEDGMENT

This work was financially supported by the NNSF of China (21575116, 51473136 and 21675129), the Natural Science Foundation Project of CQ CSTC (cstc2017jcyjA1305), the China Postdoctoral Science Foundation (2016M602626) and the Fundamental Research Funds for the Central Universities (XDJK2017C023).

REFERENCES

(1) Clark J. L.; Cho S.; Rubenstein A. H.; Steiner D. F. *Biochem. Biophys. Res. Commun.* **1969**, *35*, 456-461.

(2) Fang C.; Li H. L.; Tu Y. F. *J. Electroanal. Chem.* **2016**, *781*, 322-326.

(3) Kjems L. L.; Volund A.; Madsbad S.; *Diabetologia.* **2001**, *44*, 1339-1348.

(4) Little R.R.; Rohlfing C. L.; Tennill A. L.; Madsen R. W.; Polonsky K. S.; Myers G. L.; *Clin. Chem.* **2008**, *54*, 1023-1026.

(5) Thomas A.; Brinkkötter P. T.; Schänzer W.; Thevis M. *Forensic Toxicol.* **2017**, *35*, 106-113.

(6) Tan X.; Zhang B.; Zou G. Z. *J. Am. Chem. Soc.* **2017**, *139*, 8772-8776.

(7) Wu L.; Ding F.; Yin W. M.; Ma J.; Wang B.; Nie A. X.; Han H. Y. *Anal. Chem.* **2017**, *89*, 7578-7585.

(8) Han T. T.; Dong H.; Ren L. Lu.; Bao N.; Wu W. Z.; Ding S. N. *Chem. Commun.* **2017**, *53*, 5388-5391.

(9) Zhou Y.; Wang H. J; Zhuo Y.; Chai Y. Q.; Yuan R. *Anal. Chem.* **2017**, *89*, 3732-3738.

(10) Shan Y.; Wu H. Y.; Xiong S. J.; Wu X. L.; Chu P. K. *Angew. Chem. Int. Ed.* **2016**, *55*, 2017-2021.

(11) Hesari M. and Ding Z. F., *Acc. Chem. Res.* **2017**, *50*, 218-230.

(12) Chen Y.; Zhou S. W.; Li L. L.; Zhu J. J. *Nano Today* **2017**, *12*, 98-115.

(13) Carrara S.; Arcudi F.; Prato M.; Cola L.; *Angew. Chem. Int. Ed.* **2017**, *56*, 4757-4761.

(14) Liu J. L.; Zhao M.; Zhuo Y.; Chai Y. Q.; Yuan R.; *Chem. Eur. J.* **2017**, *23*, 1853-1859.

(15) Feng Q. M.; Guo Y. H,; Xu J. J.; Chen H. Y. *ACS Appl. Mater. Interfaces* **2017**, *9*, 17637-17644.

(16) Li X. J.; Wang Y. G.; Shi L.; Ma H. M.; Zhang Y.; Du B.; Wu D.; Wei Q. *Biosens. Bioelectron.* **2017**, *96*, 113-120.

(17) Cao W. D.; Ferrance J. P.; Demas J.; Landers J. P. *J. Am. Chem. Soc.* **2006,** *128* , 7552-7558.

(18) Cao L. Y.; Zhang R.; Zhang W. Z.; Du Z. B.; Liu C. J.; Ye Z. Q.; Song B.; Yuan J. L. *Biomaterials* **2015**, *68*, 21-31.

(19) Yang L. L.; Tao Y. Z.; Yue G. Y.; Li R. B.; Qiu B.; Guo L. H.; Lin Z. Y.; Yang H. H. *Anal. Chem.* **2016**, *88*, 5097-5103.

(20) Liu H. X.; Zhou X. M.; Liu W. P.; Yang X. K.; Xing D. *Anal. Chem.* **2016**, *88*, 10191-10197.

(21) Bi S.; Yue S. Z.; Zhang S. S. *Chem. Soc. Rev.* **2017**, *46*, 4281-4298.

(22) Wang S.; Zhang L. Q.; Wan S.; Cansiz S.; Cui C.; Liu Y.; Cai R.; Hong C. Y.; Teng I-T.; Shi M. L.; Wu Y.; Dong Y. Y.; Tan W. H. *ACS Nano* **2017**, *11*, 3943-3949.

(23) Yin, P.; Hariadi, R.; Sahu, S.; Choi, H. M. T.; Park, S. H.; LaBean, T. H.; Reif, J. H. *Science* **2008**, *321*, 824-826.

(24) Li D. D.; Cheng W.; Li Y. J.; Xu Y. J.; Li X. M.; Yin Y. B.; Ju H. X.; Ding S.J. *Anal. Chem.* **2016**, *88*, 7500-7506.

(25) Shin J. S.; Pierce N. A. *J. Am. Chem. Soc.* **2004,** *126* , 10834-10835.

(26) Yang X. L.; Tang Y. A.; Mason S. D.; Chen J. B.; Li F. *ACS Nano* **2016**, *10*, 2324-2330.

(27) Zhang L.; Niu W. X.; Gao W.Y.; Qi L.M.; Lai J.P.; Zhao J.M.; Xu G. B.; *ACS Nano* **2014**, *8*, 5953-5958.

(28) Radi, A. E.; Sánchez, J. L. A.; Baldrich, E.; O'Sullivan, C. K. *J. Am. Chem. Soc.* **2006**, *128*, 117-124.

(29) Wang H. J.; Yuan Y. L.; Zhuo Y.; Chai Y. Q.; Yuan R. *Anal. Chem.* **2016**, *88*, 2258-2265.

(30) Habtamu H. B.; Sentic M.; Silvestrini M.; Leo L. D.; Not T.; Arbault S.; Manojlovic D.; Sojic N.; Ugo P. *Anal. Chem.* **2015**, *87*, 12080-12087.

(31) Luo Y. Q.;, Liu T.; Zhu J. M.; Kong L. Y.;, Wang W.; Tan L. *Anal. Chem.* **2015**, *87*, 11277-11284.

(32) Duan H.; Huang X. L.; Shao Y.N.; Zheng L. Y.; Guo L.; Xiong Y. H. *Anal. Chem.* **2017**, 89, 7062-7068.

For TOC only